Final Version published in Computer Graphics Forum (Volume 38, 2019, number 1, pp. 549-563) available at https://doi.org/10.1111/cgf.13591

A Probabilistic Steering Parameter Model for Deterministic Motion Planning Algorithms

Philipp Agethen[1,2] † Felix Gaisbauer[1,2] Enrico Rukzio[2]‡

[1]Daimler AG Forschungs- und Entwicklungszentrum Ulm, Wilhelm-Runge-Str. 11, 89081 Ulm, Germany
[2]Ulm University, James-Franck-Ring, 89081 Ulm, Germany

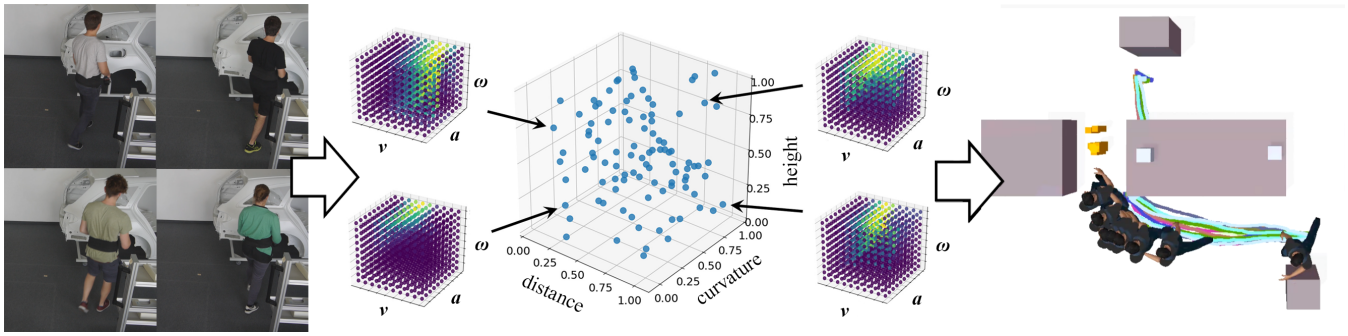

Figure 1: *Pipeline of proposed approach; Left: steering parameter estimation using a motion capture database; Center: derived probabilistic motion model containing statistically distributed steering parameters; Right: resulting motion variants.*

Abstract

The simulation of two-dimensional human locomotion in a bird's-eye perspective is a key technology for various domains to realistically predict walk paths. The generated trajectories, however, are frequently deviating from reality due to the usage of simplifying assumptions. For instance, common deterministic motion planning algorithms predominantly utilize a set of static steering parameters (e.g., maximum acceleration or velocity of the agent) to simulate the walking behavior of a person. This procedure neglects important influence factors, which have a significant impact on the spatio-temporal characteristics of the finally resulting motion - such as the operator's physical conditions or the probabilistic nature of the human locomotor system. In order to overcome this drawback, this paper presents an approach to derive probabilistic motion models from a database of captured human motions. Although being initially designed for industrial purposes, this method can be applied to a wide range of use-cases while considering an arbitrary number of dependencies (input) and steering parameters (output). To underline its applicability, a probabilistic steering parameter model is implemented, which models velocity, angular velocity and acceleration as a function of the travel distances, path curvature and height of a respective person. Finally, the technical performance and advantages of this model are demonstrated within an evaluation.

CCS Concepts

•***Computing methodologies*** → ***Modeling and simulation;*** *Model development and analysis; Animation;*

1. Introduction

Various domains ranging from video games [ASK15] over crowd simulation [VDBSGM11] to industrial production planning [IPO17, ia17] utilize two-dimensional motion planning algorithms to predict and analyze walk paths. Even though these applications differ in their scope, they nevertheless share the same goal

† e-mail: philipp.agethen@uni-ulm.de
‡ e-mail: enrico.rukzio@uni-ulm.de

Final Version published in Computer Graphics Forum (Volume 38, 2019, number 1, pp. 549-563) available at https://doi.org/10.1111/cgf.13591

to accurately reflect reality in order to increase the user experience or to draw conclusions from the simulation.

For automotive production planning, however, the outcomes of industrial simulation software are increasingly deviating from reality due to the use of simplifying assumptions [AOGR16]. Namely, these tools predominantly apply two-dimensional path planning algorithms to calculate the shortest, collision-free path between two assembly tasks [MM15]. Based on this trajectory, a so-called motion model consisting of multiple steering parameters (e.g., maximum acceleration or velocity) is utilized to animate the assembly operator along the path. Furthermore, the travel time between both assembly tasks is estimated using this model, which is the key performance indicator for planning and assessing industrial workplaces. These parameters, however, are fixed for each route and do not consider important influence factors. Additionally, by using identical steering parameters for multiple executions of the same walking task, the probabilistic nature of the human locomotor system (see [MC12]) is neglected. In contrast to this development, recent trends such as mass-customization and Industry 4.0 are leading to a growing number of different product variants. As each product variant is inevitably linked to a unique assembly sequence on the shop floor, the need for adequate simulation approaches is currently rising.

In order to overcome this drawback, this paper presents an approach to set up probabilistic motion models, containing statistically distributed steering parameter variations. Therewith, state of art motion planning algorithms are able to generate realistic and variant-rich motions, ultimately reducing the deviation between artificial and captured trajectories. The introduced principle can be used for a wide range of use-cases while taking into account arbitrary influence factors. Subsequently, this universally applicable methodology is implemented for the above mentioned use-case of automotive production planning. The resulting set of steering parameters statistically manipulates velocity, angular velocity and acceleration as a function of the travel distance, height of person and path curvature. In particular, the three main technical contributions of this paper are:

1. A generic approach to generate probabilistic motion models from a database of captured trajectories.
2. The adaption of this principle to the use-case of automotive production planning.
3. The implementation of the probabilistic motion model.

The remainder of the paper is structured as follows: first, the state of art in the context of deterministic and statistical motion synthesis and steering parameter estimation is reviewed. Second, an approach is introduced to enable deterministic motion planning algorithms to consider statistically distributed motion variations. In order to implement this principle for industrial purposes, a large number of human walking trajectories is captured using an OptiTrack motion capture system. Subsequently, a probabilistic motion model is presented, being derived from this database. Having introduced the novel approach, its applicability and technical performance is assessed in a representative experiment, inspired by an assembly situation. The paper concludes with an assessment and outlook on further optimizations.

2. Related Work

The approach presented in the following builds upon three main research areas: deterministic motion synthesis, statistical motion synthesis and steering parameter fitting algorithms.

Deterministic motion synthesis: Two-dimensional motion planning algorithms are generally utilized to generate trajectories between a starting and an end point, which fulfill certain constraints. These constraints, which are strongly affecting the behavior of the agent (e.g., path shape, velocity profile or turning speed), are usually chosen with regard to the respective use-case and physical characteristics to be modeled. Within this work, this parametrization is further referred to as motion model. In contrast to statistical algorithms, deterministic approaches are based on analytical models. Therefore, deterministic motion planning algorithms are leading to identical results, when being executed multiple times with similar input parameters. For simulating human walking, their scope of application includes, but is not limited to crowd simulations [VDBSGM11], video games [ASK15] as well as industrial walk path simulation [IPO17].

In general, the process of two-dimensional motion planning can be modeled using different concepts: While approaches like [HNR68] try to compute a collision-free path on a global level, others navigate using local motion planners [Rey99]. In principle, algorithms which belong to the former category incorporate the entire environment, hence generating global optimal solutions (collision free trajectories). In contrast, the latter only guarantees local optimality while inducing minor computational costs. Additionally, various hybrid solutions combine both approaches by utilizing a global path planning algorithm to compute a collision-free reference path, which is subsequently traversed using a local motion planner (see [LLA02, LCH03]). Since the local motion planner might reshape the initially computed path, the parametrization or motion model therefore essentially influences the spatio-temporal properties of the resulting trajectory.

Literature presents several algorithms and approaches for local as well as for global motion planning. In general, previous work in this area can be divided into approaches using cell decomposition techniques (e.g., [HNR68, NKT10]) and potential fields [GBLV15]. Furthermore, Velocity Obstacle methods (see [FS98, VDBSGM11]) have recently received significant attention for local motion planning. Other works present steering behavior approaches [Rey99], genetic algorithms [HYXM04] or neural networks [GKG95] in order to generate valid trajectories. Furthermore, Montemerlo et al. [MBB*08] present a method to compute a collision-free path while simultaneously considering motion constraints on a global level.

Even though multiple works present approaches for statistical path planning such as probabilistic roadmaps (see [LPW79, oSY83]), Rapidly Exploring Random Trees (see [LaV98]) and randomized models [HKLR02], none of these concepts introduce a comparable probabilistic motion model or address the vagueness of locomotion in general. Rather, the probabilistic principles are selected in order to handle the complexity of the search problem and are therefore and predominantly applied within high dimensional spaces (e.g., within robotics). Consequently, phenomena related to

Final Version published in Computer Graphics Forum (Volume 38, 2019, number 1, pp. 549-563) available at https://doi.org/10.1111/cgf.13591

the statistical nature of human motion - like spatio-temporal variations - and their implications on two-dimensional simulation of single subjects are not in scope of literature yet.

Statistical motion synthesis: Unlike the mentioned deterministic approaches, statistical counterparts are based on the assumption that the human locomotor system comprises an infinite number of styles and postures. Moreover, it is postulated that different executions of one motion primitive show an intrinsic relationship, which can be approximated using statistical models [MC12, DMHF16]. Based on these assumptions, various approaches targeting fully-articulated human motion have been presented ranging from Hidden Markov Models [TH00, Bow00] to Gaussian Process Dynamical Models [WFH08]. Furthermore, multiple works (see [BH00, LWS02]) combine deterministic methods with statistical models. More recently, Min and Chai [MC12] present an approach, probabilistically synthesizing fully-articulated human motion based on motion capture data. Their work is extended by Du et al. [DMHF16] transferring the approach to scenarios related to assembly workshops. Furthermore, Manns et al. investigate the influence of input data to the effectiveness of this approach [MOM16] and point out the considerable requirements in both quality and quantity for adapting the methodology to common shop-floor motions [MMM16].

Besides simulating the motion of each limb, others present various approaches for modeling and analyzing the stochasticity of human motion in the context of crowds. Wang et al. [WOO17, WOO16] propose a semantic metric to evaluate crowds and path patterns using Bayesian models. Based on similar techniques, the same authors automatically recognize activities and anomalies in videos [WO16] , while Yi et al. [YLW15] estimate statistically distributed travel times. Furthermore, Musse et al. [MCJ12] present an approach to quantitatively compare crowd using histograms, which contain informations on the local velocity distribution. Finally, Yi et al. utilize Convolutional Neural Network [YLW16] to predict pedestrian behaviors in crowded scenes.

This representative sample of works illustrates the capability to cover all the full spectrum of the human locomotor system. However, current approaches are either limited to fully-articulated motions or to the use-case of two-dimensional crowd simulation. For two-dimensional motion planning of single subjects, such models are not in scope of literature so far. Therefore, this paper bridges the gap between probabilistic approaches targeting fully-articulated human motion and two-dimensional motion planning by statistically modeling steering parameters of arbitrary deterministic motion planners.

Steering parameter fitting: In order to establish a data-driven motion model, adequate steering parameters have to be extracted from motion capture data. For two-dimensional applications, parameter estimation through optimization is a commonly used technique. These approaches compare real-world observations of human motion with synthetically generated counterparts utilizing use-case specific metrics. Subsequently, the simulation parameters are modified until the respective metric converges to a minimum, thus aligning simulation and reality. Literature presents multiple approaches (see [GvdBL*12, POO*09, LCL07]), comparing captured and synthesized two-dimensional trajectories. Moreover, other publications such as [LJK*12] and [SKFR09] offer the possibility to calibrate and compare various algorithms based on experimental datasets. In this context, Berseth et al. [BKHF14] investigate the relationship between a steering algorithm's parameters and its performance. Finally, Wolinski et al. [WJGO*14] propose a holistic approach to automatically calibrate a given steering algorithm to a given trajectory.

This paper incorporates the inspiring works of Wolinski et al. [WJGO*14] and Berseth et al. [BKHF14] to automatically extract steering parameters from real world observations, however, the main idea is extended to further consider statistically distributed variables.

3. Simulating Statistically Distributed Human Motions Using Deterministic Motion Planning Algorithms

This paper presents a data-driven motion model for arbitrary motion planning algorithms, which is built upon a database of captured walking trajectories. In general, the introduced model P_{Prob} can be regarded as a probabilistic function between a set of dependency parameter d_j (e.g., height of person or length of a walk path) and a motion planner's steering parameters p_i. Note that throughout the paper, P_{Prob} is regarded as a black-box which can only be controlled by means of manipulating the respective dependencies. Using the introduced methodology, state of the art motion planning algorithms can be extended to consider the probabilistic nature of the human locomotion - irrespective of their actual internal implementation. As a consequence, the deviation between reality and simulation can be reduced. This concept is described in the following.

Fig. 2 illustrates the main idea of this novel approach: in contrast to well-established motion models consisting of n static steering parameters p_i, this paper presents a data-driven motion model P_{Prob} statistically manipulating these variables depending on various influence factors d_j. Note that p_i is subsequently utilized to parametrize the deterministic motion planning algorithm A. The paper's main idea is derived from the fact, that, for instance, a person's maximum velocity varies widely conditioned by the curvature of the walk path. Consequently, when applying fixed p_i for each locomotion task disregarding those influence parameters, actual walk paths may deviate considerably from their simulated counterparts [AOGR16]. Moreover, by incorporating the idea of [WJGO*14, BKHF14] of fitting motion models to real world observations, P_{Prob} can be precisely calibrated to actual human motions.

In order to further take into account the probabilistic nature of the human locomotor system, this principle is extended to statistically steering parameter variations. In particular, it is assumed that locomotion properties (such as velocity or acceleration) for multiple executions of one walking task show an ambiguous behavior, even when being performed by the same person. This circumstance can be traced back to the fact that the human locomotor system comprises an infinite number of different motion variants [MC12]. Consequently, the delta between a set of captured trajectories stemming from one walking task and their artificial counterparts can be further reduced by means of modeling p_i statistically.

In order to develop an approach implementing both mentioned

Final Version published in Computer Graphics Forum (Volume 38, 2019, number 1, pp. 549-563) available at https://doi.org/10.1111/cgf.13591

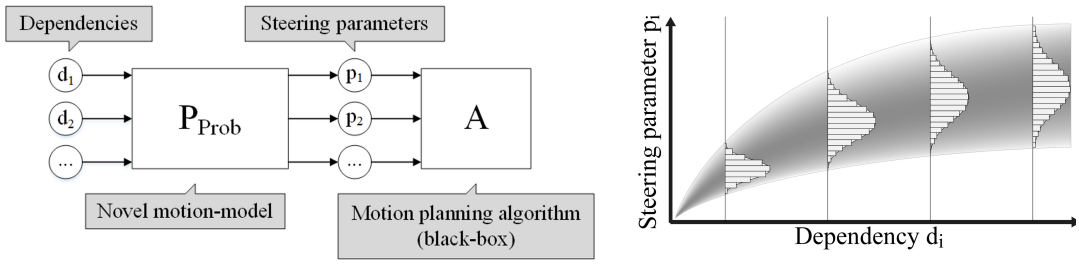

Figure 2: *Left: concept of probabilistic motion model P_{Prob}. n arbitrary steering parameters p_i are statistically manipulated depending on m influence factors d_j. Right: illustration of the probabilistic function between a pair of p_i and d_j.*

aspects, a formal deduction of P_{Prob} is initially introduced. According to Wolinski et al. [WJGO*14], a parametrized motion planning algorithm can be denoted as a function mapping the current positions $\vec{x}(t)$ of an agent to the following timestamp $t+1$ while taking into account all steering parameters p_i (see Equation 1). On this basis, the definition is extended by introducing P_{Prob} describing the statistical relationship which is specified in Equation 2. Using this novel motion model, the initial definition ultimately results in 3.

$$\vec{x}(t+1) = A(\vec{x}(t), p_i) \tag{1}$$

$$p_i = P_{Prob}(d_j) \tag{2}$$

$$\vec{x}(t+1) = A(\vec{x}(t), P_{Prob}(d_j)) \tag{3}$$

4. Generation of a Probabilistic Motion Model for Deterministic Motion Planning Algorithms

In order to generate P_{Prob} from a comprehensive database of captured walking trajectories, the following gives a detailed overview of the necessary steps, which are explained for the steering parameter velocity v, acceleration a and angular velocity ω. Moreover, the dependencies length l and curvature c of the walk path and the height h of the respective person are taken into account. Consequently, Equation 2 results in:

$$(v, a, \omega)^T = P_{Prob}(l, c, h)^T \tag{4}$$

Note that, the introduced principle is generic and can be easily adapted to various parameters.

4.1. Deduction of an Experimental Setup

First of all, the characteristics of a representative workplace have to be analyzed, in order to comply with automotive production planning. For this purpose, $\approx$ 3200 actual walk paths were initially investigated with respect to their planned distance. Note that the distances are clustered according to intervals being defined within the Methods-Time Measurement system. Fig. 3 shows the resulting frequencies. It can be seen, that 75% of all walk paths are below or around 2 *m*. Assuming a cutoff-value of 5%, the maximal distance to be consider for further investigation is 4 *m*. This circumstance can be traced back to the fact, that routes between car and material supply are optimized by the production planning departments in order to reduce unproductive task times. Therefore routes usually do not exceed distances of half the assembly station size - which is approximately 6 *m* to 8 *m* for cars.

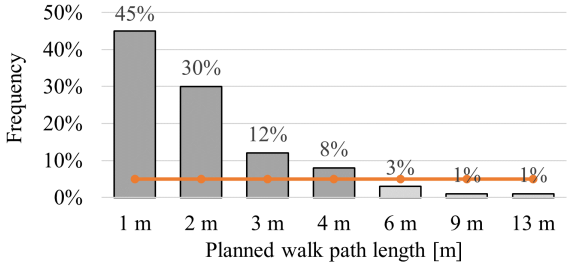

Figure 3: *Frequency of distances for 3197 planned walk paths in an actual automotive final assembly line.*

4.2. Generation of a Database

Having determined the characteristics of a representative workplace, next, a comprehensive database of walking motions is generated. In the context of this paper, walk paths stemming from 30 participants serve as a baseline for the subsequent steps. In particular, the full-body movements of a person are monitored using an OptiTrack system (update rate 120 Hz). Based on the gathered datasets, the skeleton's center of mass (COM) is subsequently projected onto the floor plane in order to be compatible with two-dimensional motion planning algorithms.

To cover a large motion variety and to consider, both intra- and inter-subject variance, 30 participants were recruited for the experiment. The group comprised 25 male and 5 female being aged from 19 to 59 ($\mu = 26.46$, $\sigma = 7.50$) with a height ranging from 1.65 m to 1.90 m ($\mu = 1.78$ *m*, $\sigma = .07$ *m*) and an average body weight of 75.15 kg ($\sigma = 13.09$ kg, $min = 50$ *kg* and $max = 110$ *kg*). Furthermore, the group of participants consisted of 23 students and 7 production planning employees. In order to not obstruct the walking style, participants wore their own clothing and shoes. None of the participants reported vision or balance disorders.

As the proposed P_{Prob} models steering parameter as a function of the trajectory length and curvature, the database has to further contain multiple variants of walk paths lengths and turning angles.

Consequently, walking was recorded in two independent scenarios: linear walking along a straight line as well as non-linear around a pole. The former consisted of 8 equally distributed distances between .5 m and 4.0 m (see Section 4.1) whereas the latter comprised 4 varying turning angles (i.e., $45^\circ - 180^\circ$). To further measure the influence of the traveling distance on turning behavior, each of the four configuration comprised two variants of 3 m and 4 m (see left side of Fig. 4). All scenarios included 3 min of walking between start and the target point at self-selected speed. Within both scenarios, the order of walk path length and turning angle was randomized. Having reached the target, the participant returned to start after standing still for 5 s. This procedure was repeated before again walking to the target. These two phases before and after each locomotion cycle subsequently served as distinctive landmarks to reliably distinguish between walking towards the target and returning to the initial position.

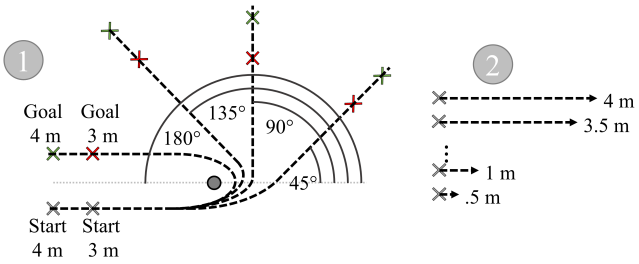

Figure 4: *Setup of first experiment: (1) participants walked around a pole for varying angles and distances. (2) the identical group walked along a straight line in a range between .5m and 4.0m.*

Having performed the described procedure, the 30 participants generated a comprehensive database consisting of 1848 point-to-point walk paths with a total length of over 4.97 km.

4.3. Generation of a Discrete Suitability Map

In order to statistically simulate human locomotion, the relationship between different values of steering parameters and their suitability to reproduce a given reference trajectory is modeled next. The resulting function can be subsequently used to make prediction about adequate p_i configurations, when planning an unknown motion. In particular, different values in a certain steering parameter configuration space (hereinafter also referred to as SPCS) are utilized to re-simulate each captured walk path. For this purpose, an arbitrary motion planning algorithm is initialized using a p_i-vector from the configuration space. Next, an artificial walk path is synthesized, while taking into account all obstacles and constraints of the scene. Having generated a valid path, the deviation from its captured counterpart is computed. Finally, this step is repeated using varying steering parameters p_i, until all possible combinations are assessed. The outcome of this procedure is a discrete map, describing the suitability of the SPCS, to reproduce a certain walk path.

Within this paper, this step is implemented as follows: A virtual representation of the captured scene is initially created, using the knowledge about start and target position. A virtual agent comprising of a global and local motion planner is subsequently utilized to simulate the motion between the two captured points. In

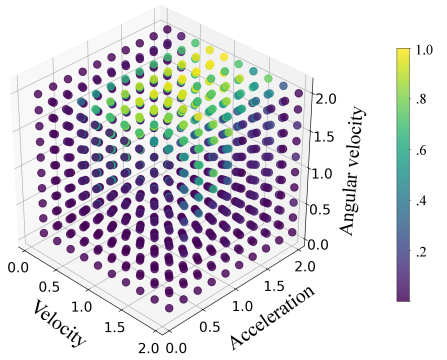

Figure 5: *Exemplary three-dimensional discrete suitability map for the steering parameters v, a and ω: The color yellow depicts areas with a high suitability to reproduce a given trajectory, whereas blue represents error-prone regions.*

particular, a LazyTheta* [NKT10] (cell size .01 m) in combination with [Rey99] was used to simulate walking motions. In order to further consider acceleration, the rate of velocity change is constrained. Same applies for angular velocity, whereas no global threshold is used. In contrast, a linear relationship between velocity and maximum angular velocity is defined - as indicated by [COMP13]. Following Berseth et al. and Wolinski et al. [WJGO*14, BKHF14], the resulting artificial walk path is compared with the corresponding captured trajectory T_k by means of the sum of absolute Euclidean distances between the reference and the simulated walk path (normalized with the length of the reference path). Equation 5 depicts m_{Euclid}. Note that other metrics can be utilized as a measurement for assessing the quality of a certain steering parameter vector.

$$m_{Euclid} = \frac{\sum \left\| T_k(t+1) - A\left(\vec{x}(t), P_{Prob}(l,c,h)^T\right)\right\|}{\|T_k\|} \tag{5}$$

In order to obtain steering parameter combinations from the SPCS, different algorithms such as greedy approach or simulated annealing can be utilized [WJGO*14]. In this paper, those values are determined by means of discretizing the space within a certain range. These ranges are chosen to be $v \in [.1, 2.0]\frac{m}{s}$, $a \in [.1, 2.0]\frac{m}{s^2}$ and $\omega \in [.1, 2.0]$. The latter value describes the gradient of limiting angular velocity line. Respectively, this procedure results in a three dimensional configuration space - according to following equations:

$$V \times A \times \Omega = \{(v,a,\omega) | v \in V, a \in A, \omega \in \Omega\} \tag{6}$$

$$V = \{(.1 + i * .21)\frac{m}{s} | i \in 0,1,2,...,9\} \tag{7}$$

$$A = \{(.1 + i * .21)\frac{m}{s^2} | i \in 0,1,2,...,9\} \tag{8}$$

$$\Omega = \{(.1 + i * .21) | i \in 0,1,2,...,9\} \tag{9}$$

Having simulated and assessed each combination, a n-dimensional discrete map of similarity scores is obtained for a

given trajectory. Note that the map may comprise different number of dimensions, which correspond to the number of steering parameters p_i. Fig. 5 shows an exemplary three dimensional suitability map for one trajectory (values of m_{Euclid} have been normalized to 1 and subtracted from 1 in order to better highlight suitable regions). The color yellow represents areas with an overall high suitability to reproduce the respective trajectory. This step can also be seen on the top of Fig. 7 for a two dimensional SPCS.

4.4. Construction of a Dependency Blending Space

Third, the procedure of generating suitability maps is repeated for each trajectory within the database (see Fig. 6). The outcome of this step are 1848 discrete maps, modeling the individually suitability to reproduce the respective trajectory. In general, the characteristics of those maps vary vastly depending on the underling motion. For instance, a map being generated for a route of 4 m will significantly deviate from a counterpart, representing a rather short walk path (e.g., .5 m). This is due to the fact, that participants reach higher walking speeds when traveling longer distances. This circumstance will also be reflected in the corresponding suitability map. Besides the trajectory and its properties, the physical characteristics of the respective participant may also have a systematic impact on the resulting suitability distribution.

As a consequence, it is essential to preserve these informations about trajectory, respective person or other circumstances for downstream processes. In the context of this paper, the dependencies d_j are chosen to be length l of the walk path and the height h of the respective person. Moreover, the curvature c of the trajectory is also considered, which is defined as the the sum of curvatures at each point c_i along the curve, being normalized by l: $c = \sum \frac{|c_i|}{l}$. For this purpose, interpolating splines (function *UnivariateSpline*, $k = 5$ [JOPo01]) are utilized. Note that the captured COM trajectory is smoothed using a Gaussian filter (function gaussian_filter1d, sigma = 2 [JOPo01]) in order to minimize the influence of gait induced jerks. Having determined the respective d_j-parameter, each of the 1848 maps is linked to its corresponding dependency vector.

Finally, a so-called dependency blending space (DBS) is constructed, which aligns the 1848 d_j-vectors according to their respective values. As each entry is linked to its corresponding suitability map, grids stemming from, for example, tall and smaller persons are thus clustered. Fig. 6 shows such an exemplary DBS comprising 100 suitability maps. It can be seen, that the data-points in the DBS are defined by their d_j-values. Moreover, Fig. 6 illustrates that each element is linked its individual suitability map, which vary statistically with respect to their position in the DBS.

The main benefit of utilizing a dependency blending space, is that it allows an efficient interpolation, using nearest neighbor search operations (i.e., k-nearest neighbors). Consequently, it is possible to efficiently obtain a desired number of similar suitability maps for a given d_j-vector. Since the accuracy of the KNN interpolation strongly relies on the density of the reference datasets, the method proposed by Kovar and Gleicher [KG04] is further applied. As a result, a homogenized DBS comprising 5000 entities is utilized throughout the paper.

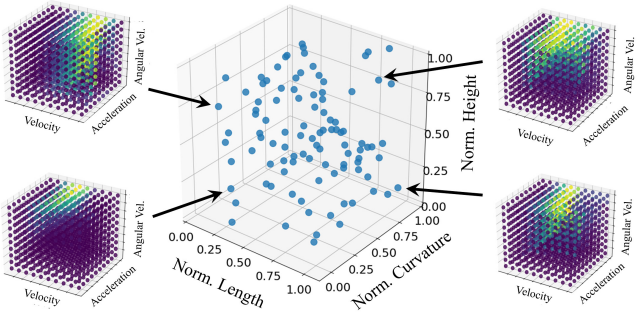

Figure 6: *Exemplary three dimensional dependency blending space for $d_j = (l,c,h)^T$, containing 100 suitability maps, which are aligned according to their d_j-value.*

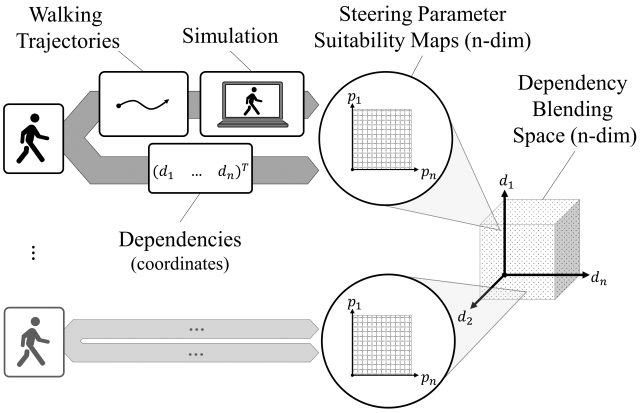

Figure 7: *Principle to generate P_{Prob}: 1) a n-dimensional suitability map is generated for each trajectory within a given database. 2) Each of the suitability maps is linked to its corresponding d_j-vector. 3) These linked maps are finally utilized to construct a m-dimensional dependency blending space.*

5. Usage of a Probabilistic Motion Model During Run-Time

Having generated the DBS, this model can be used to generate statistically distributed steering parameters during run-time. In order to obtain plausible steering parameter samples, a two-staged interpolation process is proposed. Fig. 9 depicts this procedure. In a first step, the k-nearest neighbors in the DBS are obtained for a desired d_j (function *KDTree* [PVG*11]). Based on the distances in the DBS, the simultaneously obtained k maps are hence weighted linearly and interpolated. The outcome of this process is one novel suitability map for a given d_j.

Fig. 8 shows the outcome of this procedure in form of eight 3D-grids. The color yellow represents areas with an overall high suitability to reproduce the underlying trajectories. In contrast to the assumption of previous work concerning steering parameter fitting, it can be seen that all maps do not show one single global optimum but ambiguous results. Moreover, these models further contain the

Final Version published in Computer Graphics Forum (Volume 38, 2019, number 1, pp. 549-563) available at https://doi.org/10.1111/cgf.13591

initially captured variance since the sweet spots show a blurred behavior with no sharp borders.

Next, this discrete grid is further interpolated using radial basis functions [JOPo01]. After applying the RBF-interpolation, a given map shows a continuous behavior in terms of v, a and ω. Finally, the normalized suitability function is interpreted as a probability density function f. This enables the utilization of an acceptance-rejection algorithm to draw random observations from the distribution. Acceptance-rejection sampling is a type of Monte Carlo method and is performed by uniformly sampling a point $\vec{x}_{rand} = (v_{rand}, a_{rand}, \omega_{rand})$ in the 3-dimensional parameter space of the proposal distribution. Additionally, a value r in the range from zero to the maximum of the probability density function is sampled uniformly: $r \sim U(0, \max(f))$. If the obtained value r is less than or equal to the value of the distribution function evaluated at $\vec{x}_{rand}$ (i.e., if $r \leq f(\vec{x}_{rand})$), the point is accepted, otherwise rejected. In this case, the whole procedure is repeated until one point is finally accepted. Consequently, areas with high suitability scores show a higher likelihood to be drawn from the statistical model than those with lower values.

The main advantage of using a sampling-based method to obtain steering parameter from a continuous suitability function is, that it reproduces the ambiguous nature of human locomotion. For instance, a function being constructed using 100 maps comprises several local maximums and areas with an overall-high suitability (see Fig 8). These areas might potentially lead to enhanced results for a given trajectory, compared to the function's global maximum. The acceptance-rejection approach allows to draw samples from these areas being rated marginally lower. Please note, that it is nevertheless possible to utilize the interpolated function's global maximum for use-cases, which do not consider stochastic effects.

Performed on an Intel i7-6820HQ with 2.70 GHz, the two-staged interpolation algorithm in combination with the acceptance-rejection sampling algorithms allows the generation of novel steering parameter samples in approximately 100 ms (100 neighbors). This value can be regarded to be sufficient when simulating one or two assembly operators. Note that it is possible to significantly reduce computation time by means of parallelization.

6. Further Possible Areas of Application for the Proposed Approach

In general, besides modeling two-dimensional trajectories of single subjects, the presented approach can be applied to a wide range of use-cases. The only prerequisite is, that the utilized motion generation algorithms can be externally controlled via a set of scalar parameters.

For two-dimensional motion planning, a second prominent area of application is the domain of crowd simulation - as discussed in Section 2. In contrast to the presented approach, here, the similarity of motions has to be analyzed using metrics, being more adequate for this respective use-case (such as *vorticity* or *fundamental diagram* [WJGO*14]). Furthermore, varying motion planning approaches (e.g., [VDBSGM11]) comprising different steering parameter have to be utilized.

Increasing the motion's dimensionality, the animation of a digital human model along a multidimensional path is a second possible field, which could directly benefit from the proposed approach. For instance, a reach motion of a three-dimensional character and its spatio-temporal characteristics, can be calibrated to a given set of captured data. For this purpose, the hand's velocity can be varied in order to analogously generate suitability maps. Note that the utilized metrics, on the one hand, can address one single limb (e.g., wrist). On the other hand, it is also possible to evaluate the pose of the fully-articulated character or the naturalness of its trajectories (e.g., smoothness).

Regardless of the application, the presented generic principle enables a calibration of a probabilistic parameter model to a given dataset of real world observations. Consequently, a deterministic, state of the art algorithm can be extended to consider the intrinsic stochasticity of human motion, without adapting its implementation. The utilized metric, comparing artificial and captured motion has to be chosen with respect to the simulation's scope. For instance, motion execution time, smoothness of trajectory, naturalness of pose or shape similarity can be thus enhanced.

7. Evaluation of Prediction Quality

In order to measure the performance of the proposed probabilistic motion model, both the novel and a state of art approach are compared with captured human motions. In the context of this evaluation, the prediction quality is measured by means of travel time differences. In particular, Δt is used due to the significant importance of task durations for manufacturing and production planning. In particular, when assessing the efficiency of an assembly line, the ratio of value-adding and non-value-adding task times is regarded. The non-value-adding portion is usually comprised to a large extent by walking. Thus, when optimizing an assembly line, minimizing travel times is essential.

7.1. Participants

For this experiment 10 participants, differing from the population of the first experiment (see section 4.2) were recruited. This group comprised 9 male and 1 female being aged from 21 to 40 ($\mu = 27.80$, $\sigma = 6.08$) with a height ranging from 1.60 m to 1.98 m ($\mu = 1.79\ m$, $\sigma = .12\ m$) whereas the mean weight was 76.20 kg ($\sigma = 14.18$ kg, $min = 60\ kg$ and $max = 105\ kg$). None of the participants reported vision or balance disorders.

7.2. Apparatus

In order to obtain a representative test case, two setups inspired by a workplace within an assembly line were chosen. As depicted in Fig. 10, scenario 1 comprised one car body and three racks being positioned on one side, whereas the latter included two shelves (height of 1.0 m and .6 m), each containing a single screw. The first rack (number 3) had a distance of .7 m to the interaction point 1, whereas the other two racks had an offset of 2.2 m and 2.9 m, spanning an angle of approximately 90°. Furthermore, within scenario 2, the car was placed between two racks. Moreover, the point of assembly was defined to be at the car's bonnet (distances 2.0 m

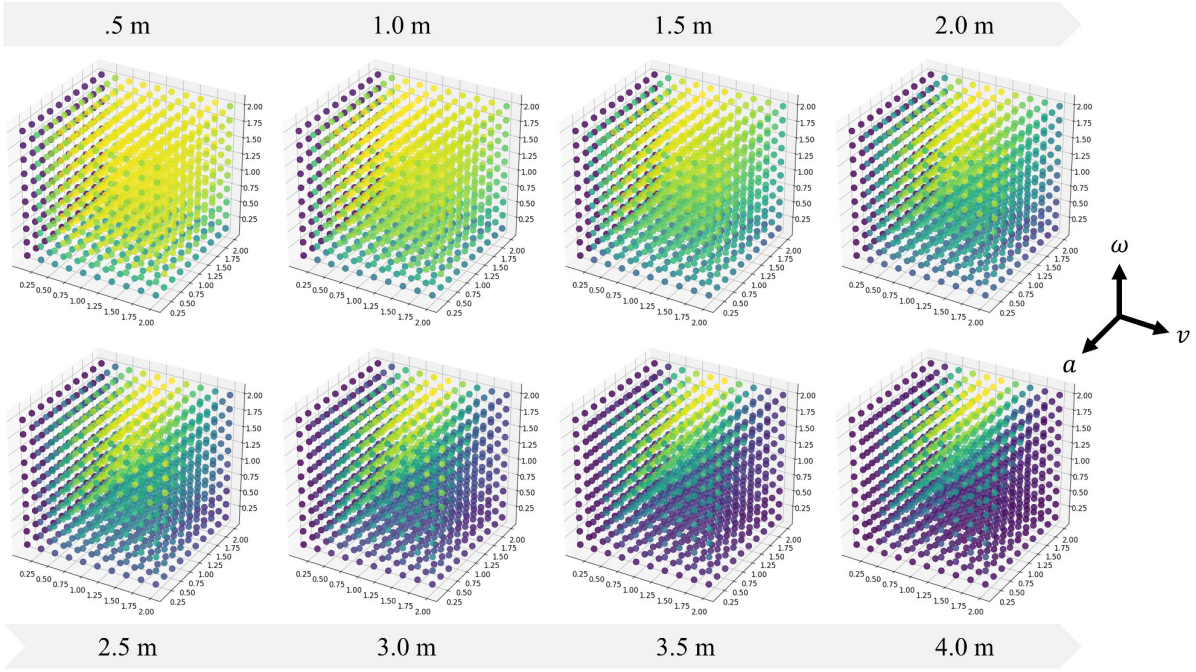

Figure 8: *Eight resulting three-dimensional suitability maps for $l \in [.5\,m, \ldots, 3.0\,m]$, $c = 0$ and $h = 1.80m$. The color yellow depicts areas with an overall high suitability to reproduce the corresponding trajectories.*

for rack 1 and 2.4 *m* for rack 2). Using these setups, the predominant proportion of walk paths occurring in a final assembly workplace, including obstacle avoidance, could be covered (see Section 4.1).

In order to observe the motion of each participant, the center of mass was monitored using an HTC Vive tracking system (update rate 60 Hz) [ABT*02]. For this purpose, a controller was placed on the front side in center of the participant's hip (i.e., umbilicus) with the help of an elastic belt. The COM was subsequently derived for each participant as the extension of the controller's z-axis while

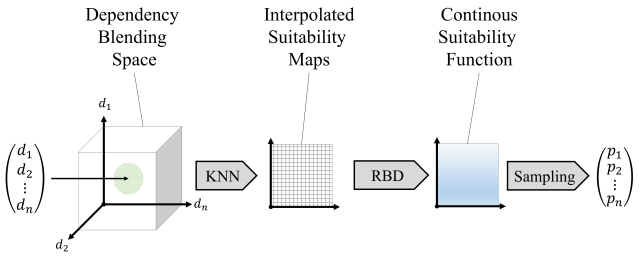

Figure 9: *Procedure to generate statistically distributed p_i-samples: 1) the d_j-vector is utilized to determine k similar suitability maps in the dependency blending space. 2) a novel map is generated by means of KKN interpolation. 3) the discrete map is further interpolated using radial basis functions. 4) an adequate p_i- sample is obtained by means of acceptance-rejection sampling.*

taking into account half of the torso depth and the distance between controller and skin. By analogy with section 4.2, the gathered datasets were identically processed and segmented.

7.3. Procedure

During both scenarios, a representative list of assembly tasks was carried out 10 times. For scenario 1, each set included 11 walk paths between the three racks and the final assembly point: first, each participant was asked to start at rack 2 and successively carry and fasten the two screws to the car at a self-selected speed. Next, the same procedure was repeated for number 3 and finally for rack 1. Note that each of the six screws had to be assembled individually in order to maximize the amount of walking. Analogously, scenario 2 comprised 6 walk paths: 2 between rack 1/2 and assembly point 3 and 2 between both racks while avoiding the car.

Having captured and extracted all COM trajectories in both scenarios, the set of assembly tasks were simulated while taking into account the knowledge about captured start and end point including position and dimension of all obstacles. Subsequently, three motion models were utilized to independently simulate the identical walk paths.

P_{Stat} : In order to allow a direct comparison between the proposed probabilistic approach P_{Prob} and an equivalent static motion model P_{Stat}, the global optimum in terms of $p_i = (v, a, \omega)^T$ was determined according to [WJGO*14]. For this purpose, the 1848 point-to-point walk paths being captured in Section 4.2 were utilized. Moreover, Equation 5 was chosen to compare captured and synthetic walk paths whereas simulated annealing was

Final Version published in Computer Graphics Forum (Volume 38, 2019, number 1, pp. 549-563) available at https://doi.org/10.1111/cgf.13591

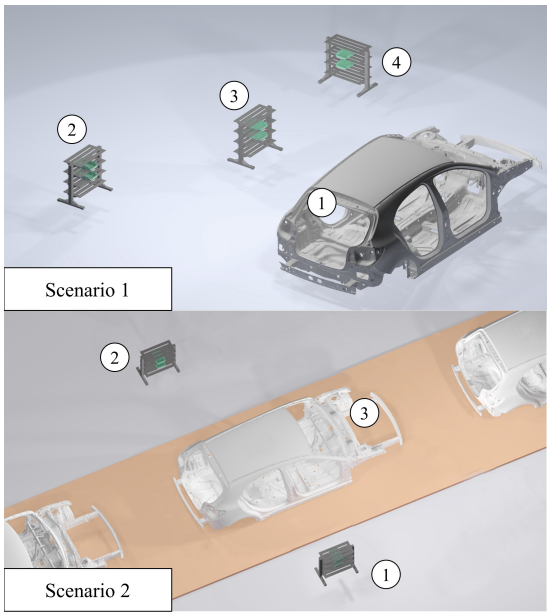

Figure 10: *Setup of second experiment: a participant had to successively fetch and tighten six screws which were stored in three racks on a car body-in-white for 10 times.*

utilized to determine the optimal steering parameter configuration [WJGO*14]. As the database for the static motion model and the proposed probabilistic approach is identical, P_{Stat} represents the static counterpart of P_{Prob}. Using the captured trajectories, the optimization process determined an optimal steering parameter configuration of $v = .94\ m/s$, $a = 1.58\ m/s^2$ and $\omega = 1.79$ for P_{Stat}.

P_{Prob} : Furthermore, P_{Prob} was set up as described above using the database from Section 4.2. Afterwards, P_{Prob} was utilized to individually draw one parameter vector for each walk path. For this purpose, the distance and curvature of the LazyTheta* algorithm (smoothed, function gaussian_filter1d, sigma = 2 [JOPo01]) was utilized in order to approximate the expected dependency parameters. Moreover, the height of the respective person was loaded from the annotated dataset. Next, $d_j = (l, c, h)^T$ was used to interpolate the probability density function for the expected walk path as described above ($k = 100$ for KNN). One parameter sample was afterwards generated from this function using the acceptance-rejection sampling algorithm. Finally, the sampled p_i-vector initialized the motion planner for simulating this particular walk path.

P_{Adapt} : With regard to P_{Stat}, the proposed approach comprises two significant modifications: the d_j-dependent generation of a suitability function and the probabilistic sampling. In order to differentiate and to quantify their respective influence on the overall-performance, a third intermediate motion model (i.e., P_{Adapt}) is set up. P_{Adapt} represents the deterministic counterpart of P_{Prob}. In particular, no acceptance-rejection sampling is utilized to generate adequate p_i-values from the interpolated suitability function. Instead, steering parameter vectors are obtained by means of determining the global maximum.

7.4. Results

Scenario 1: During scenario 1, more than 1984 point-to-point walk paths with an overall-length of 4.06 km could be gathered. Fig. 11 depicts the delta of the overall walking duration Δt between the captured and the simulated walk paths using the tested motion models. In particular, boxplots and their corresponding histograms give an overview of the temporal deviation between the simulated and captured walk paths. It can be seen that none of the measurements shows a normal distribution. Instead, a positive skew is observed. A performed shapiro-wilk test (SPSS) underlines these finding, scoring low p-values, which converge to zero. The mid-section of Fig. 11 lists the outcome of this test and further descriptive statistics.

It can be seen, that P_{Stat}, representing the static state of art motion model, shows a median Δt value of .514 s. Moreover, the 25^{th} and 75^{th} percentiles account for .262 s / .838 s, which corresponds to an interquartile range of .576 s. The 5^{th} and 95^{th} percentiles are at .052 s and 1.464 s. Furthermore, the deterministic P_{Adapt} motion model, comprising a d_j-dependent steering parameter generation, points out an improved prediction quality. As listed in Fig. 11, the median error decreases to .475 s, while the 25^{th} and 5^{th} percentiles are .235 s / .046 s. The 75^{th} and 95^{th} percentile show a reduced error of .772 s / 1.350 s. Finally, the probabilistic motion model P_{Prob} points out a further reduced deviation between simulation and reality. It can be seen, that the median error accounts for .453 s, while the 25^{th} and 75^{th} percentiles are .231 s and .747 s. The 5^{th} and 95^{th} percentile lay at .040 s and 1.212 s.

In order to further statistically compare the non-normal datasets, a parametric wilcoxon signed-rank test is chosen (SPSS) comprising a confidence level of 95%. The bottom of Fig. 11 gives an overview of the obtained results. It becomes apparent, that each tested pair of motion models ($P_{Stat} \leftrightarrow P_{Adapt}$, $P_{Adapt} \leftrightarrow P_{Prob}$ and $P_{Stat} \leftrightarrow P_{Prob}$) indicate a statistically significant difference between both measurements (i.e., $p = .000$ to .015). Moreover, each test's power is calculated using G*Power [FELB07], pointing out sufficient values (i.e., $1 - \beta = .951$ to 1.000) in all cases - except $P_{Adapt} \leftrightarrow P_{Prob}$.

Scenario 2: Furthermore, the group of participants generated 3.26 km of walk paths in the context of scenario 2. As shown in Fig. 12, the Δt error distribution for each tested motion model is non-normal ($p = .000$). Regarding P_{Stat}, it can be seen, that the median of is .850 s, while the 25^{th} and 75^{th} percentiles are at .462 s / 1.247 s. Furthermore, the results being obtained using P_{Adapt}, indicate an improved resemblance to the baseline. In particular, the median deviation is reduced to .771 s, whereas both quartiles lay at .436 s and 1.138 s. Analogous to scenario 1, the probabilistic motion model P_{Prob} scores the lowest Δt values. Similar to the previous scenario, the performed statistical analysis reveals significant differences for each pair of motion models. As the archived power is above the desired level of .800 (except $P_{Adapt} \leftrightarrow P_{Prob}$) , again, the all thus obtained outcomes are significant.

7.5. Discussion

P_{Stat} vs. P_{Adapt}: Comparing the deterministic motion models, which only differ in terms of d_j-adaptive steering parameter gen-

eration, in both scenarios, it can be seen that P_{Adapt} shows a significantly improved resemblance to reality ($p = .002$, $1-\beta = .951$ / $.953$). For scenario 1, the median error is reduced by 8%, while the 75^{th} and 95^{th} percentiles are decreased by 10% and 8%. Scenario 2 indicates a similar enhancement. In particular, the delta for the median error is 9%, while the 75^{th} and 95^{th} percentiles are lowered by 6% and 9%. Summarizing these findings, it can be confirmed, that a adaptive p_i-approximation significantly improves the prediction quality (i.e., temporal deviations) of deterministic motion models.

As the training datasets for P_{Stat} and P_{Adapt} are identical, this circumstance can be traced back to the fact, that the DBS sorts the database of suitability maps according to their dependency parameters. Consequently, it is ensured that only adequate datasets are utilized, when generating a novel suitability map. For instance, the interpolation of a suitability function for a long walk path would lead to inferior results, if maps are used, which were generated using shorter distances (e.g., .5 m). As the d_j-adaptive steering parameter generation rules out such unwanted effects, it can be concluded, that exclusively the presented technique reduces the deviation from reality.

P_{Adapt} vs. P_{Prob}: As mentioned above, the difference between motion models P_{Adapt} and P_{Prob} is the utilization of differing techniques to obtain p_i from the interpolated suitability function. In particular, the global optimum is determined for P_{Adapt}, whereas P_{Prob} uses probabilistic acceptance-rejection sampling. The findings for both scenarios point out, that the latter increases the prediction quality, even though the power of .687 and .629 (i.e., $< .800$) does not allow to draw statistically significant conclusions. In particular, a reduced median error of 5% / 6% can be observed. Same applies for the 25^{th} and 75^{th} percentiles, ranging between 3% and 11% - for both scenarios.

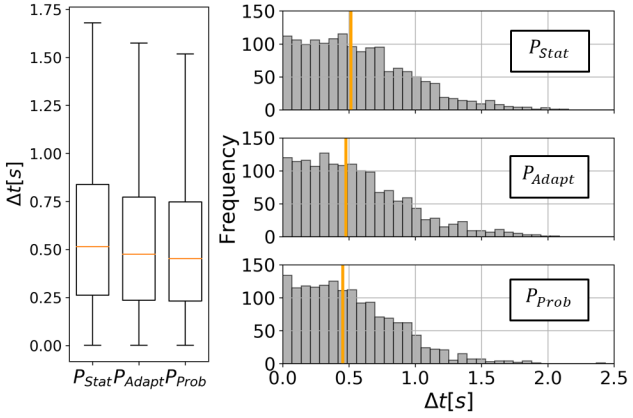

	P_{Stat}	P_{Adapt}	P_{Prob}
25th Percentile	.262 s	.235 s	.231 s
50th Percentile	.514 s	.475 s	.453 s
75th Percentile	.838 s	.772 s	.747 s
p (Shapiro-Wilk)	.000	.000	.000

	$P_{Stat} \leftrightarrow P_{Adapt}$	$P_{Adapt} \leftrightarrow P_{Prob}$	$P_{Stat} \leftrightarrow P_{Prob}$
p (Wilcoxon)	.001	.015	.000
Power	.951	.687	1.000

Figure 11: *Scenario 1: resulting statistics of Δt for the tested motion models: histogram and boxplots (top) . Descriptive statistics (center) and outcomes of performed statistical analysis (bottom).*

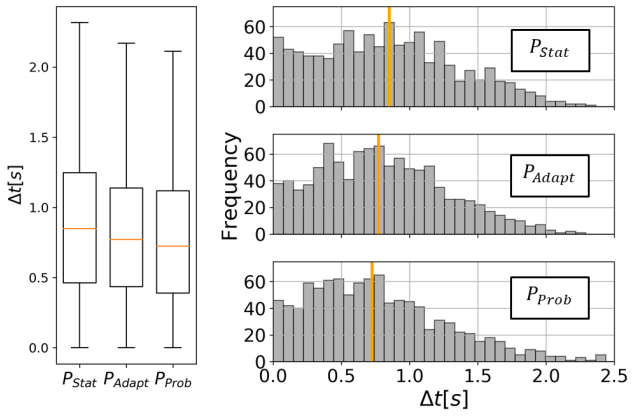

	P_{Stat}	P_{Adapt}	P_{Prob}
25th Percentile	.462 s	.436 s	.390 s
50th Percentile	.850 s	.771 s	.724 s
75th Percentile	1.247 s	1.138 s	1.118 s
p (Shapiro-Wilk)	.000	.000	.000

	$P_{Stat} \leftrightarrow P_{Adapt}$	$P_{Adapt} \leftrightarrow P_{Prob}$	$P_{Stat} \leftrightarrow P_{Prob}$
p (Wilcoxon)	.001	.023	.000
Power	.953	.629	.992

Figure 12: *Scenario 2: resulting statistics of Δt for the tested motion models.*

On the one hand, the evident improvements can be exclusivity attributed to the different sampling strategy, which allows the generation of statistically distributed parameter variations. Consequently, the consideration of inter- and intra-subject variability outperforms its deterministic counterpart. The main reason for this is, that for P_{Adapt}, motion executions which deviate from the mean are inevitably leading to a discrepancy between simulation and reality. On the other hand, a possible reason for the test's low power is, that highly inadequate areas of the multidimensional suitability function, possess values, which are marginally greater than zero. As a consequence, the probability of drawing p_i from those unsuitable areas is unequal to zero. Such sampled outliers are inevitably affecting the resulting error distribution. One possible countermeasure is the utilization of a threshold or to adapt the suitability function (e.g., exponentiation). Nevertheless, it can be concluded that the novel motion model increases the prediction quality.

P_{Stat} vs. P_{Prob}: Unifying both preceding comparison, it can be concluded that P_{Prob} outperforms the state of the art motion model in both test-scenarios. In particular, statistically significant differences are found ($p = .000$, $1-\beta = 1.000$ / $.992$), which correspond to a decreased median deviation from reality by 12% / 15%. The remaining percentiles range between 10% and 16% for both scenar-

ios. Consequently, the combination of adaptive steering parameter estimation and probabilistic sampling is leading to a superior degree of realism. This circumstance can be exclusively attributed to the proposed approach, as the underlying training datasets are identical for each model.

Summarizing it is to be noted, that the presented evaluation conveys a consistent picture for both associated scenarios. In particular, the relative delta between the compared motion models is nearly constant. This circumstance leads to the conclusion, that neither the setup, nor the shape of the walk paths or the presence of obstacles (see Fig.10) correlate with the overall-performance. Consequently, the presented probabilistic approach is proven to be applicable to varying environments.

Finally, the obtained findings are transferred to the use-case of automotive production planning. Assuming an exemplary assembly workplace with a cycle time of 100 s and a proportion of 20% walking, the proposed approach would reduce the error between simulation and reality by approx. $2-3$ s - per car being produced. This underlines the potential of utilizing probabilistic motion models for industrial applications.

8. Analysis of Model and Influence Parameters

Having assessed the overall-performance of the approach, finally, the underlying techniques and the different influence parameters are investigated in detail.

8.1. Analysis of Model Parameters

First, the contribution of all six dependency and steering parameters is investigated. For this purpose, each parameter is individually removed, thus resulting in six independent sub-models: $P_{Prob,l}$, $P_{Prob,c}$, $P_{Prob,h}$, $P_{Prob,v}$, $P_{Prob,a}$ and $P_{Prob,w}$. For instance, $P_{Prob,l}$ comprises two dependency (i.e., curvature and height of participant) and all three steering parameters. Compared to P_{Prob}, however, $P_{Prob,l}$ does not take the length of the planned walk path into account. $P_{Prob,v}$, in turn, solely models acceleration and angular velocity as a function of all three dependencies. Having constructed six sub-models, the trajectories being captured in the context of scenario 1 are subsequently used to analyze the individual contribution of each parameter.

Fig. 13 illustrates the results of this analysis. Analogous to the previous section (see Fig. 11), P_{Prob} scores a median Δt error of .453 s. The sub-model $P_{Prob,l}$, neglecting the length of the planned walk paths, increases this error to .506 s. Furthermore, the individual removal of curvature and height of the assembly operator leads to an inferior prediction quality: .542 s and .471 s. With regard to the steering parameters, similar results can be observed. In particular, neglecting velocity, acceleration or angular velocity increases Δt: .545 s, .507 s and .495 s.

Summarizing the findings, the results point out, that curvature has the largest contribution to the model's prediction quality. A possible reason for this circumstance is, that the assembly related character of scenario 1 leads to walk paths with a predominantly curved form. Furthermore, the rather short routes inhibit a stronger

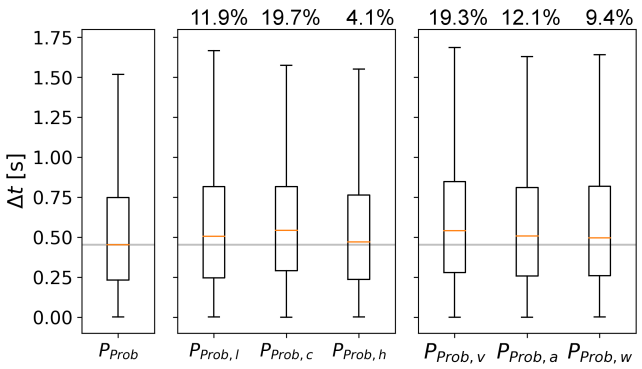

Figure 13: *Analysis of influence of each steering and dependency parameter on the overall-result.*

impact of l and h on the overall-results. With regard to the steering parameters it is to be noted, that the consideration of velocity leads to the highest reduction in terms of Δt. Even though showing a varying contribution, it can be concluded, that each introduced parameter improves the overall-results

8.2. Analysis of Dependency Blending Space

Second, the appropriateness of both chosen interpolation methods is investigated. First, the KNN technique is compared to existing suitability maps (ground truth). For this purpose, one respective entity is removed from the DBS. Afterwards, the proposed KNN approach is utilized to mimic this suitability map for the corresponding d_j. The outcome of the interpolation process is subsequently compared with the excluded ground truth by means of subtracting the suitability scores (median). This process is successively repeated for each of the 5000 entries. In total, the KNN-interpolation is able to reproduce suitability scores with following statistics: $\mu = -.434\%$ and $\sigma = 5.104\%$. Given the wide range of variability in terms of human motion, an error of $< 5\%$ is regarded to be acceptable. However, more advanced interpolation techniques, as discussed in [FHKS12], could potentially lead to further improved results.

Additionally, the utilized radial basis functions are analyzed. Analogous to the previous evaluation, one entry is removed from the suitability map, and subsequently regarded as ground truth. Afterwards, the RBF interpolation is applied to the remaining datapoints, in order to reconstruct the removed baseline. As the outcome of this process might vary depending on the position in the grid, this procedure is repeated for 100 randomized indices. The outcome of this step are 100 measurement points, whose median is subsequently analyzed. Being repeated for each of the 5000 maps, a neglectful mean deviation of $-.048\%$ ($\sigma = .172\%$) can be observed. Consequently, the RBD interpolation can be regarded as well suited.

As k - i.e., number of suitability maps, being used for interpolation - is known to have a considerable impact on the outcome of KNN-approaches, this parameter is further investigated. In particular, scenario 1 is evaluated using different numbers of neighbors,

Final Version published in Computer Graphics Forum (Volume 38, 2019, number 1, pp. 549-563) available at https://doi.org/10.1111/cgf.13591

while the temporal deviation from the captured reference motions is measured. Fig. 14 shows the result for $k \in 10, 20, 50, 100, 200, 500$. Most notably, a negative correlation between k and Δt can be observed. While $k = 10$ points out a large deviation from the baseline (i.e., median of 1.425 *s*), this error is reduced by 27% for $k = 20$. For 50 neighbors the results point out a reduction to .609 *s*, whereas the mean time needed to interpolate the suitability maps nearly doubles. This trend continues for $k = 100$, which results in $\Delta t = .453$ *s* (see previous section) coupled with a processing time of 38.4 *ms*. For higher k-value a slight improvement in terms of Δt can be observed (i.e., 17% and 3%), however, at the expense of computational efforts. In particular, this value rises to 184.7 *ms* for $k = 500$.

The results demonstrate, that the model's prediction quality is considerably affected by k, as is converges. Consequently, it is advisable to chose high k-values since this procedure apparently inhibits the influence of local outliers. Moreover, the number of utilized suitability maps increases the inherited motion variance of the interpolated function. The evaluation reveals, that given the utilized DBS (i.e., 5000 up-sampled entities), $k > 50$ generates reasonable results. However, considering the exponentially rising interpolation times, $k = 100$ is the optimal compromise between Δt and computational efforts.

8.3. Analysis of Suitability for Simulating Longer Distances

In order to further underline the generality of the proposed approach, third, an independent probabilistic model is constructed to simulate long distances. Similar to the previous sections, a group of 10 individuals was recruited. This group showed following properties: age between 21 to 40 ($\mu = 26.30$, $\sigma = 5.01$) with a height ranging from 1.75 m to 1.90 m ($\mu = 1.81$ *m*, $\sigma = .05$ *m*). This group walked distances of 10, 25 and 50 meters, while being video recorded. For this purpose a *Panasonic Lumix DMC-G6* was used resulting in a frame rate of 25 Hz and in a resolution of 1920x1080. Using this apparatus, it was possible to precisely determine travel times using the video footage. In particular, the exact frames of the double-stance posture before and after locomotion were used. The group of participants performed each of the three walk paths in a randomized order. This procedure was repeated four times, thus leading to four walk paths for each distance. Subsequently, the dataset was split-up into to halves. One half was used to train a probabilistic motion model, whereas the other part served as test data. Furthermore, P_{Prob} models acceleration and velocity as a function of participant height and distance.

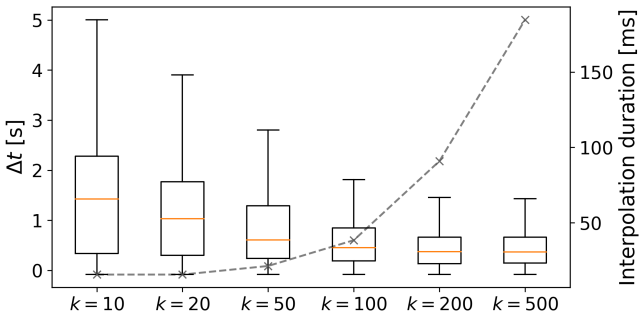

Figure 14: *Analysis of correlation between number of neighbors k and the overall-result / interpolation time.*

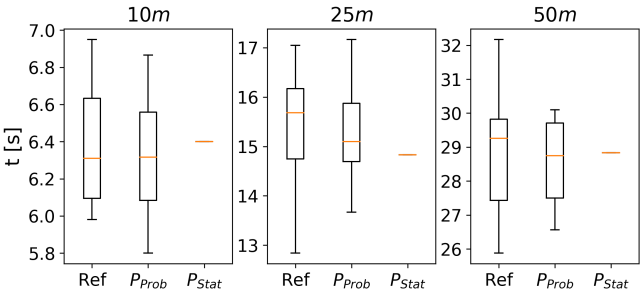

Figure 15: *Comparison of P_{Prob} and P_{Stat} in the context of 10 m, 25 m and 50 m walk paths.*

Fig 15 summarizes the travel times distributes for 10 *m*, 25 *m* and 50 *m*. *Ref* illustrates the captured durations of the test dataset, while P_{Prob} and P_{Stat} represent the simulated counterparts. For 10 *m*, the reference median travel time is 6.310 *s*, while its interquartile range (IQR) is .538 *s*. The probabilistic model matches this behavior by predicting a median duration of 6.317 *s* (IQR .475 *s*). The global optimum results in 6.400 *s*. For 25 *m*, a similar situation can be observed. The baseline points out a median travel time of 15.685 *s* (IQR 1.428 *s*), which is reproduced by P_{Prob}: median 15.100 and IQR 1.183. P_{Stat} predicts a duration of 14.833 *s*. For the longest distance, the participants' median travel time is 29.260 *s* (IQR 2.395 *s*). The artificial walk paths account for 28.750 *s* (IQR 2.208 *s*) and 28.833 *s*.

The results mainly demonstrate, that on the one hand, both models predict the median travel time with a low deviation $< 5\%$. On the other hand, however, the comparable IQR of P_{Prob} underlines, that the proposed approach precisely reproduces the vagueness in human motion - even in the context of long distances. This behavior, however, is neglected when using P_{Stat}. Please note that this preliminary evaluation does not allow to draw statistically significant conclusions due to the limited number of test data. Nevertheless the results can be interpreted as a strong indicator of the model's suitability to adequately simulate long distances. This further underlines the generality of the proposed approach.

9. Conclusion

This paper introduced an approach to generate a probabilistic motion model from real-world observations to simulate variant-rich motion trajectories using arbitrary state of art motion planning algorithms. The generic principle can be applied to any steering parameter and any influence factor. Furthermore, this approach is not solely limited to the field of two-dimensional walking simulation but can be transferred to a wide range of even higher dimensional problems, which are related to the simulation of human motion (e.g., grasping trajectories for human limbs).

Using this methodology, a model is implemented, which manipulates velocity, acceleration and angular velocity depending on the

Final Version published in Computer Graphics Forum (Volume 38, 2019, number 1, pp. 549-563) available at https://doi.org/10.1111/cgf.13591

walk path length, curvature and height of the respective person. Based on two assembly-related experimental setups, this approach is compared with two deterministic motion models. The evaluation reveals two main advantages which contribute to an increased prediction quality:

1. The consideration of dependencies without probabilistic sampling for generating steering parameter significantly increases the resemblance to real world observations.
2. The enhanced prediction quality can be further improved by means of probabilistically sampling steering parameters.

Even though the novel approach offers several evident benefits, the current implementation can still be optimized and extended. For instance, the consideration of other influence factors such as cognitive load, gaze or distractions could potentially lead to enhanced results. Moreover, future work will also prove that the generic principle can be adopted to other use-cases such as three-dimensional grasping simulation while taking into account a larger number of steering and influence parameters.

References

[ABT*02] AUVINET B., BERRUT G., TOUZARD C., MOUTEL L., COLLET N., CHALEIL D., BARREY E.: Reference data for normal subjects obtained with an accelerometric device. *Gait & Posture 16*, 2 (Oct. 2002), 124–134. 8

[AOGR16] AGETHEN P., OTTO M., GAISBAUER F., RUKZIO E.: Presenting a Novel Motion Capture-based Approach for Walk Path Segmentation and Drift Analysis in Manual Assembly. *Procedia CIRP 52* (2016), 286–291. 2, 3

[ASK15] ALGFOOR Z. A., SUNAR M. S., KOLIVAND H.: A comprehensive study on pathfinding techniques for robotics and video games. *International Journal of Computer Games Technology 2015* (Jan. 2015). 1, 2

[BH00] BRAND M., HERTZMANN A.: Style machines. In *Proceedings of the 27th annual conference on Computer graphics and interactive techniques* (2000), ACM Press/Addison-Wesley Publishing Co., pp. 183–192. 3

[BKHF14] BERSETH G., KAPADIA M., HAWORTH B., FALOUTSOS P.: Steerfit: Automated parameter fitting for steering algorithms. In *Proceedings of the ACM SIGGRAPH/Eurographics Symposium on Computer Animation* (Aire-la-Ville, Switzerland, Switzerland, 2014), SCA '14, Eurographics Association, pp. 113–122. 3, 5

[Bow00] BOWDEN R.: Learning statistical models of human motion. In *IEEE Workshop on Human Modeling, Analysis and Synthesis, CVPR* (2000), vol. 2000. 3

[COMP13] CIRIO G., OLIVIER A. H., MARCHAL M., PETTRE J.: Kinematic evaluation of virtual walking trajectories. *IEEE Transactions on Visualization and Computer Graphics 19*, 4 (April 2013), 671–680. 5

[DMHF16] DU H., MANNS M., HERRMANN E., FISCHER K.: Joint Angle Data Representation for Data Driven Human Motion Synthesis. *Procedia CIRP 41* (2016), 746 – 751. 3

[FELB07] FAUL F., ERDFELDER E., LANG A.-G., BUCHNER A.: G* power 3: A flexible statistical power analysis program for the social, behavioral, and biomedical sciences. *Behavior research methods 39*, 2 (2007), 175–191. 9

[FHKS12] FENG A., HUANG Y., KALLMANN M., SHAPIRO A.: An analysis of motion blending techniques. In *Motion in Games* (Berlin, Heidelberg, 2012), Kallmann M., Bekris K., (Eds.), Springer Berlin Heidelberg, pp. 232–243. 11

[FS98] FIORINI P., SHILLER Z.: Motion planning in dynamic environments using velocity obstacles. *The International Journal of Robotics Research 17*, 7 (1998), 760–772. 2

[GBLV15] GASPARETTO A., BOSCARIOL P., LANZUTTI A., VIDONI R.: Path Planning and Trajectory Planning Algorithms: A General Overview. In *Motion and Operation Planning of Robotic Systems*, Carbone G., Gomez-Bravo F., (Eds.), vol. 29. Springer International Publishing, Cham, 2015, pp. 3–27. 2

[GKG95] GLASIUS R., KOMODA A., GIELEN S. C.: Neural Network Dynamics for Path Planning and Obstacle Avoidance. *Neural Networks 8*, 1 (1995), 125–133. 2

[GvdBL*12] GUY S. J., VAN DEN BERG J., LIU W., LAU R., LIN M. C., MANOCHA D.: A statistical similarity measure for aggregate crowd dynamics. *ACM Transactions on Graphics 31*, 6 (Nov. 2012), 1. 3

[HKLR02] HSU D., KINDEL R., LATOMBE J.-C., ROCK S.: Randomized Kinodynamic Motion Planning with Moving Obstacles. *The International Journal of Robotics Research 21*, 3 (Mar. 2002), 233–255. 2

[HNR68] HART P., NILSSON N., RAPHAEL B.: A Formal Basis for the Heuristic Determination of Minimum Cost Paths. *IEEE Transactions on Systems Science and Cybernetics 4*, 2 (1968), 100–107. 2

[HYXM04] HU Y., YANG S. X., XU L.-Z., MENG M. Q. H.: A knowledge based genetic algorithm for path planning in unstructured mobile robot environments. In *2004 IEEE International Conference on Robotics and Biomimetics* (Aug 2004), pp. 767–772. 2

[ia17] IMK AUTOMOTIVE: ema. www.imk-ema.com/, 2017. 1

[IPO17] IPO.PLAN: IPO.Log. www.ipoplan.de/software/ipolog/, 2017. 1, 2

[JOPo01] JONES E., OLIPHANT T., PETERSON P., OTHERS: *SciPy: Open source scientific tools for Python*. 2001. 6, 7, 9

[KG04] KOVAR L., GLEICHER M.: Automated extraction and parameterization of motions in large data sets. In *ACM Transactions on Graphics (TOG)* (2004), vol. 23, ACM, pp. 559–568. 6

[LaV98] LAVALLE S. M.: *Rapidly-exploring random trees: A new tool for path planning*. Tech. rep., Computer Science Dept., Iowa State University, 1998. 2

[LCH03] LI T.-Y., CHEN P.-F., HUANG P.-Z.: Motion planning for humanoid walking in a layered environment. In *2003 IEEE International Conference on Robotics and Automation* (Sept 2003), vol. 3, pp. 3421–3427 vol.3. 2

[LCL07] LERNER A., CHRYSANTHOU Y., LISCHINSKI D.: Crowds by Example. *Computer Graphics Forum 26*, 3 (Sept. 2007), 655–664. 3

[LJK*12] LEMERCIER S., JELIC A., KULPA R., HUA J., FEHRENBACH J., DEGOND P., APPERT-ROLLAND C., DONIKIAN S., PETTRE J.: Realistic following behaviors for crowd simulation. In *Computer Graphics Forum* (2012), vol. 31, Wiley Online Library, pp. 489–498. 3

[LLA02] LIM CHEE WANG, LIM SER YONG, ANG M.: Hybrid of global path planning and local navigation implemented on a mobile robot in indoor environment. IEEE, pp. 821–826. 2

[LPW79] LOZANO-PEREZ T., WESLEY M. A.: An algorithm for planning collision-free paths among polyhedral obstacles. *Communications of the ACM 22*, 10 (Oct. 1979), 560–570. 2

[LWS02] LI Y., WANG T., SHUM H.-Y.: Motion texture: a two-level statistical model for character motion synthesis. In *ACM transactions on graphics (ToG)* (2002), vol. 21, ACM, pp. 465–472. 3

[MBB*08] MONTEMERLO M., BECKER J., BHAT S., DAHLKAMP H., DOLGOV D., ETTINGER S., HAEHNEL D., HILDEN T., HOFFMANN G., HUHNKE B., JOHNSTON D., KLUMPP S., LANGER D., LEVANDOWSKI A., LEVINSON J., MARCIL J., ORENSTEIN D., PAEFGEN J., PENNY I., PETROVSKAYA A., PFLUEGER M., STANEK G., STAVENS D., VOGT A., THRUN S.: Junior: The stanford entry in the urban challenge. *Journal of Field Robotics 25*, 9 (2008), 569–597. 2

[MC12] MIN J., CHAI J.: Motion graphs++: a compact generative model for semantic motion analysis and synthesis. *ACM Transactions on Graphics 31*, 6 (Nov. 2012), 1. 2, 3

Final Version published in Computer Graphics Forum (Volume 38, 2019, number 1, pp. 549-563) available at https://doi.org/10.1111/cgf.13591

[MCJ12] MUSSE S., CASSOL V., JUNG C.: Towards a quantitative approach for comparing crowds. *Computer Animation and Virtual Worlds 23* (2012). 3

[MM15] MANNS M., MARTIN N. A. A.: Improving a* walk trajectories with b-splines and motion capture for manual assembly verification. *Procedia CIRP 33* (2015), 364–369. 2

[MMM16] MANNS M., MENGEL S., MAUER M.: Experimental effort of data driven human motion simulation in automotive assembly. *Procedia CIRP 44* (2016), 114–119. 3

[MOM16] MANNS M., OTTO M., MAUER M.: Measuring motion capture data quality for data driven human motion synthesis. *Procedia CIRP 41* (2016), 945–950. 3

[NKT10] NASH A., KOENIG S., TOVEY C.: Lazy Theta*: Any-angle path planning and path length analysis in 3d. In *Third Annual Symposium on Combinatorial Search* (2010). 2, 5

[oSY83] O'DUNLAING C., SHARIR M., YAP C. K.: Retraction: A new approach to motion-planning. ACM Press, pp. 207–220. 2

[POO*09] PETTRE J., ONDREJ J., OLIVIER A.-H., CRETUAL A., DONIKIAN S.: Experiment-based modeling, simulation and validation of interactions between virtual walkers. In *Proceedings of the 2009 ACM SIGGRAPH/Eurographics Symposium on Computer Animation* (2009), ACM, pp. 189–198. 3

[PVG*11] PEDREGOSA F., VAROQUAUX G., GRAMFORT A., MICHEL V., THIRION B., GRISEL O., BLONDEL M., PRETTENHOFER P., WEISS R., DUBOURG V., VANDERPLAS J., PASSOS A., COURNAPEAU D., BRUCHER M., PERROT M., DUCHESNAY E.: Scikit-learn: Machine learning in Python. *Journal of Machine Learning Research 12* (2011), 2825–2830. 6

[Rey99] REYNOLDS C. W.: Steering behaviors for autonomous characters. In *Game developers conference* (1999), pp. 763–782. 2, 5

[SKFR09] SINGH S., KAPADIA M., FALOUTSOS P., REINMAN G.: SteerBench: a benchmark suite for evaluating steering behaviors. *Computer Animation and Virtual Worlds 20*, 5-6 (Sept. 2009), 533–548. 3

[TH00] TANCO L. M., HILTON A.: Realistic Synthesis of Novel Human Movements from a Database of Motion Capture Examples. In *Proceedings of the Workshop on Human Motion (HUMO'00)* (Washington, DC, USA, 2000), HUMO '00, IEEE Computer Society, pp. 137–. 3

[VDBSGM11] VAN DEN BERG J., SNAPE J., GUY S. J., MANOCHA D.: Reciprocal collision avoidance with acceleration-velocity obstacles. In *Robotics and Automation (ICRA), 2011 IEEE International Conference on* (2011), IEEE, pp. 3475–3482. 1, 2, 7

[WFH08] WANG J., FLEET D., HERTZMANN A.: Gaussian Process Dynamical Models for Human Motion. *IEEE Transactions on Pattern Analysis and Machine Intelligence 30*, 2 (Feb. 2008), 283–298. 3

[WJGO*14] WOLINSKI D., J GUY S., OLIVIER A.-H., LIN M., MANOCHA D., PETTRE J.: Parameter estimation and comparative evaluation of crowd simulations. In *Computer Graphics Forum* (2014), vol. 33, Wiley Online Library, pp. 303–312. 3, 4, 5, 7, 8, 9

[WO16] WANG H., O'SULLIVAN C.: Globally continuous and non-markovian crowd activity analysis from videos. In *Computer Vision – ECCV 2016* (Cham, 2016), Leibe B., Matas J., Sebe N., Welling M., (Eds.), Springer International Publishing, pp. 527–544. 3

[WOO16] WANG H., ONDŘEJ J., O'SULLIVAN C.: Path patterns: Analyzing and comparing real and simulated crowds. In *Proceedings of the 20th ACM SIGGRAPH Symposium on Interactive 3D Graphics and Games* (New York, NY, USA, 2016), I3D '16, ACM, pp. 49–57. 3

[WOO17] WANG H., ONDŘEJ J., O'SULLIVAN C.: Trending paths: A new semantic-level metric for comparing simulated and real crowd data. *IEEE Transactions on Visualization and Computer Graphics 23*, 5 (May 2017), 1454–1464. 3

[YLW15] YI S., LI H., WANG X.: Pedestrian travel time estimation in crowded scenes. In *2015 IEEE International Conference on Computer Vision (ICCV)* (Dec 2015), pp. 3137–3145. 3

[YLW16] YI S., LI H., WANG X.: Pedestrian behavior understanding and prediction with deep neural networks. In *Computer Vision – ECCV 2016* (Cham, 2016), Leibe B., Matas J., Sebe N., Welling M., (Eds.), Springer International Publishing, pp. 263–279. 3

Final Version published in Computer Graphics Forum (Volume 38, 2019, number 1, pp. 549-563) available at https://doi.org/10.1111/cgf.13591